The core structure of AGN: perils of adaptive optics artifacts

SCOTT C. CHAPMAN, GORDON A. H. WALKER
University of British Columbia, Vancouver, B.C. V6T 1Z4, Canada
schapman@astro.ubc.ca, walker@astro.ubc.ca

and

SIMON L. MORRIS
Dominion Astrophysics Observatory, Victoria, B.C., Canada
simon@dao.nrc.ca

October 27, 1998

ABSTRACT

As part of a project to map nearby Seyfert galaxies in the near-IR with adaptive optics, we present high spatial resolution, near-IR images in J,H, and K of the nuclei of NGC 3227 and NGC 2992, obtained with the Adaptive Optics Bonnette (AOB) on CFHT. The $\sim$ 0.15" resolution allows us to probe structures in the core region at unprecedented scales. With NGC 3227, we are able to identify an inwards spiraling starburst in all three near-IR bands. NGC 2992 shows evidence for emission along a radio loop. Compared with HST optical images, dust obscuration becomes significantly less pronounced at longer wavelengths, revealing the true geometry of the core regions. The observed structures may help to elucidate fueling mechanisms for the central engine, as well as providing insight into the unification paradigms. The results are tempered with the discovery of AOB-related artifacts in the central arcsec of observed AGN galaxies which take on the appearance of spiral/disk structures.

1. INTRODUCTION

It is generally accepted that pronounced activity in galaxies hosting Active Galactic Nuclei (AGN) results from accretion onto a supermassive black hole. This paradigm has led to a plethora of research into AGN, of which the problems of overcoming the angular momentum barrier to fuel the nucleus and unification of the AGN types have risen to the forefront as especially vexing and controversial. Near-IR imaging has proven to be a powerful means to study these AGN problems since the dust extinction is reduced, and the contrast between the central AGN and the underlying stellar population is improved. A fresh perspective can be gained on the core regions of AGNs through the high resolution images now possible thanks to adaptive optics (AO).

We have begun a project to map nearby Seyfert galaxies in the near-IR with adaptive optics in order to study core morphologies and address possible fueling mechanisms. Here, we present observations of NGC 3227 and NGC 2992 obtained with the AO system on the 3.6 m Canada-France-Hawaii Telescope. Both galaxies live in disturbed environments:

• NGC 3227 is an SABa galaxy classified as Sy1.5, interacting with its dwarf elliptical neighbor, NGC 3226. It has been much studied in recent years as it contains many of the elements thought to be related to the formation and evolution of active nuclei: emission line regions excited by both starburst and AGN continuum, strong interaction, and a stellar bar (Gonzales Delgado & Perez 1997, Arribas & Mediavilla 1994).

• NGC 2992 is an Sa galaxy seen almost edge-on and interacting with NGC 2993. It possesses an active Seyfert nucleus classified as Sy1.9. A large and prominant dust lane runs through the center of the galaxy roughly north to south, splitting the nuclear region in two. Ulvestad and Wilson (1984) found that the radio structure of the nucleus of NGC 2992 has the shape of a "figure-8", with a maximum extent of about 2000 pc, oriented out of the plane of the galactic disk. Most of of the 6cm radio emission from the center of the galaxy arises in the loops of the figure-8 rather than in the nucleus.

2. OBSERVATIONS

The imaging observations were obtained at the CFHT in March, 1997, using the MONICA near-IR camera (Nadeau et al. 1994) mounted at the f/20 focus of the Adaptive Optics Bonnette (AOB). The detector is a Rockwell NICMOS3 array with 256x256 pixels and a 0.034"/pix scale. The CFHT AOB is based on curvature wavefront sensing (Roddier 1991), and uses a 19 zone bimorph mirror to correct the wavefront distortions. As the field size is small (9"x9"), blank sky images were taken intermitantly between science frames. On-source images were taken in a mosaic of 4 positions, alternately putting the galaxy core in each of the four quadrants of the array. Flux and PSF calibrations were performed using the UKIRT standard stars fs13 and fs25. Flat-field images were taken on the dome with the lamps turned on and off to account for the thermal glow of the telescope. The nuclei of the galaxies themselves were used as the guiding source for the AO system, a clear point source for NGC 3227 and a more extended core for NGC 2992. The natural seeing averaged 0.6"-0.8" throughout the observations resulting in relatively high strehl ratios in all bands, and FWHM of 0.14", 0.17", 0.22" at K, H, J bands respectively. At a distance of 15 Mpc for NGC 3227, 1"=76pc using $H_0 = 50$. The estimated distance of NGC 2992 at 20Mpc implies an angular scale of 100pc / 1".

3. THE COMPLETE SAMPLE

Candidate galaxies for our survey were chosen based primarily on core guidability with AOB. Our sample galaxies therefore tend to have the brightest cores amongst nearby Seyferts (though not necessarily unresolved) and may not be representative of the lower luminosity active nuclei. However, our Seyferts typically have bright X-ray flux and are perhaps the best sample with which to study the AGN phenomenon, since they are uncontaminated with borderline AGN galaxies. There are roughly equal numbers of Seyfert type 1 and 2 galaxies, since a bright extended core seems to provide a good guiding source with curvature sensing adaptive optics. We note however that the types of artifacts around the central AGN spike vary with the core morphology, and identifying physical structures is a nontrivial matter within the central arcsecond. The complete sample is presented in Table 1, along with alternate designations, redshift, filters obtained, Seyfert class (S=saturated core, U=unresolved core, R=resolved core; all Sy2 are resolved; (S) = HST saturated core); galaxy classification, and camera used: KIR or MONICA.

3.1. AOB artifacts - the difficulty of identifying physical structure

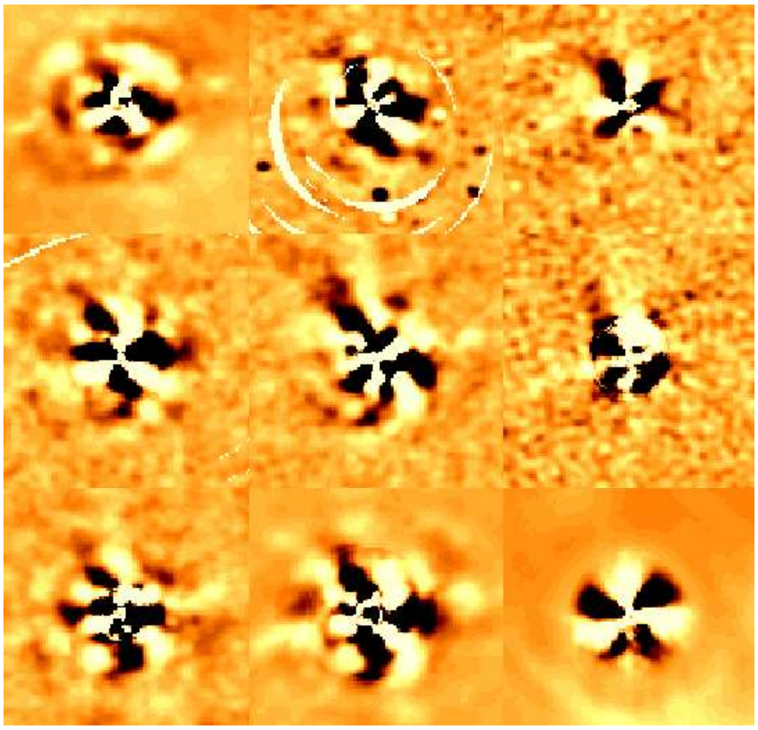

Fig. 1.— A representative sample of the cores of our Seyfert galaxies at K-band, 3.4" on a side. An elliptical isophote model has been subtracted from each. Left to right: Ic4329, Mkn1330, Mkn744, Mkn620, NGC3516, NGC3998, NGC4051, NGC4151, Mkn348

The exciting results on AGN cores emerging from AOB studies are tempered with the discovery of achromatic, AOB-related artifacts in the central arcsec surrounding the bright nuclei of observed AGN galaxies. These artifacts masquerade convincingly as the expected types of morphologies in the centers of Seyfert galaxies: small-scale spiral arms, edge-on disks or tori,

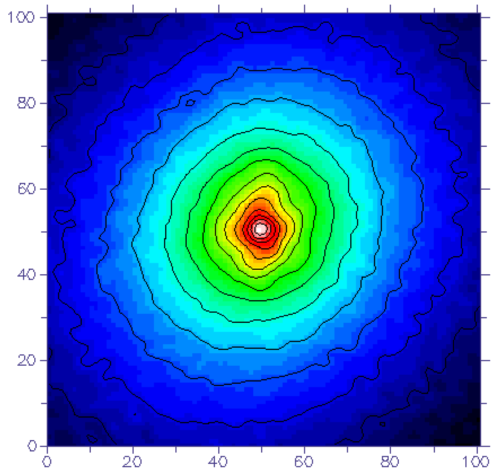

Fig. 2.— NGC3998 K-band, 3.4” on a side, raw data. A cross-type feature surrounds the nucleus, resembling spiral and torus structures.

double nuclei, and outflows. Figure 1 shows a representative sample of AGN cores. Elliptical isophotes were fit to the galaxy core region. A smooth model was then built from the resulting fit, and subtracted from the raw image. Alternatively, median filtered images were subtracted from the core with the same result. The most pronounced effect in all the raw images is an extended core to the North. Figure 1 clearly depicts that these structures exist at the same scale with similar shape and orientation relative to North, regardless of Seyfert type or distance to the galaxy. In particular NGC 3998, NGC 3516, and Mkn 348 all show a cross-like pattern suggestive of small-scale spiral arms plus a bar or edge-on torus. The K-band image of NGC 3998 is displayed in Figure 2, and shows the effect of this cross pattern artifact is significant even in the raw image. The northern component of the cross encompasses more than 10% of the peak of the central core. In the case of NGC 3227, the AOB core was compared with HST-NICMOS data (Alonso-Herrero, private communication) and the core cross pattern was found not to exist, even at very low signal levels. Note that a similar feature may have been mistakenly identified as a physical structure in NGC1068 (Rouan et al. 1998). We stress, however, that the AOB system is perfectly reliable in identifying systems such as binary stars or galaxies with true double nuclei, if the relative flux is less than a factor of 10, or if the artifact is carefully taken into account (see Knapen et al. 1997 and Lai et al. 1998 for resolved double nuclei in Mkn273 and Mkn231 respectively which appear to be real).

A technique has been developed to reconstruct the AOB PSF from the modal control used during the actual observations (Veran et al. 1998). The algorithm requires a fairly bright guiding source to accurately reproduce the PSF, and not all our galaxy cores satisfy this criterion. Reconstructed PSFs for 4 of the galaxies depicted in Figure 1 (all with bright cores), are shown in figure 3 with a smooth model subtracted. Structures are similar in scale to the actual galaxy data, showing some kind of “lobe” configuration. The actual galaxy counterparts to these

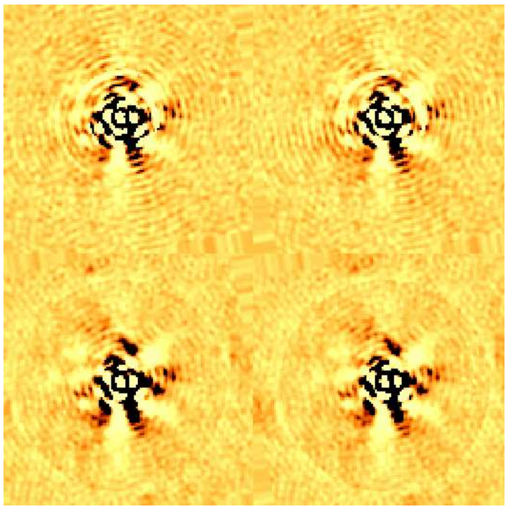

Fig. 3.— Four of the reconstructed PSFs from Figure 1 with a smooth model subtra cted (4" on a side). Structures are similar in scale to the actual galaxy data, showing some kind of "lobe" configuration. Left to right: Mkn620, NGC3998, NGC4051, NGC4151

reconstructions display a broad range in core morphology from the extremely bright pointsource in NGC 4151 to the bright but extended Seyfert 2 Mkn 620. The reconstructed PSF has essentially the same morphology in all cases, and certainly does not reproduce the actual artifact morphology in the galaxy cores. However, the reconstruction does not take into account the extended nature of the underlying galaxy and the nuclear core, and would not be expected to reproduce the artifact if it was related to this. Non-common light path to the wavefront sensor and IR array may also contribute to the discrepancy.

The structures are most prominent when a bright point source dominates the core, and is less apparent in the weaker or more extended cores, possibly indicating that the artifact is strongest when the AOB correction is at its best. The morphology is also not dependent on the camera used with AOB (both the 1k^2 pixel KIR and 256^2 pixel MONICA show identical artifacts, once the images have been rotated to the same orientation on the sky).

Although some stars imaged with AOB were reported not to show extended PSF cross-patterns, we find that the structures appear to contaminate our calibration stellar images corrected with AOB in a similar manner (Chapman et al. 1999a in preparation). Thus the extended underlying galaxy is likely not the primary cause of the cross-shaped and double/triple-lobed artifacts. Further modeling of the response of the curvature based wavefront sensing AO system is required to ascertain the root of such structures. Deconvolution techniques may be able to account for these artifacts sufficiently, once their true nature is uncovered. This will allow the central arcsecond of active galaxies to be probed with more confidence using AOB.

Table 1: The AOB observed Seyfert galaxy sample

Galaxy	Alternate	z	filters	sy class	gal type	instrument
ic 4329a	eso 445-g50	0.016	J,H,K,CO	S1	Sa,S0	KIR
mrk 1066	UGC 2456	0.012	J,H,K	2	Sc,SB0	KIR
mrk 1330	NGC 4593	0.009	J,H,K	U?1	Sb/c, SBb	KIR
mrk 3	UGC 3426	0.014	J,H,K	2	S0	KIR
mrk 620	NGC 2273	0.006	J,H,K	2	SBb,SBa	KIR
mrk 744	NGC 3786	0.010	J,H,K	U1.8(S)	Sb,Sa	KIR
mrk 766	NGC 4253	0.012	J,H,K	U1.5(S)	SBc,Sa	KIR
ngc 2639	NGC 4593	0.011	J,H,K	R1	Sb,Sa	KIR
ngc 2992		0.007	J,H,K,CO	2	Sa	KIR/MON
ngc 3516	UGC 6153	0.009	J,H,K	S1.5	S0	KIR
ngc 3998		0.008	J,H,K	U1.5	E	KIR
ngc 4051		0.002	J,H,K	S1	Sb,SBbc	KIR
ngc 4151		0.002	J,H,K	S1	Sa/	KIR
ngc 4968	ESO 508-g6	0.009	H	2	Sa/SB0a	KIR
ngc 5033		0.002	J,H,K	2		KIR/MON
ngc 5135	ESO 444-g32	0.013	K	2	Sc,SBaba	KIR
ngc 5273		0.004	H	R1.8	Sa/	KIR
ngc 3081		0.007	K	2	SBca	KIR
ngc 3393		0.012	K	2	Sa/SBa	KIR
mrk 1376	NGC 5506	0.007	J	R1.9	Sa/edge	KIR
ngc 3227	UGC 5620	0.003	J,H,K	U1.5(S)	SBa	MONICA
ngc 5548	MRK 1509	0.017	J,H,K	U1.5(S)	Sa	MONICA
mrk 348	NGC 262	0.014	H,K	2	Sa,S0a	MONICA
ngc 1068		0.003	H	2	Sb/	MONICA
ngc 7469		0.016	H	U1(S)	Sb/c	MONICA
ngc 1241		0.013	H	2	Sb/c, SBb	MONICA
ngc 1275		0.013	K	1.5	Sa/	MONICA
ngc 1386		0.002	H,K	2	Sb/c	MONICA
ngc 5728		0.005	K	2	Sb/	MONICA
ngc 5929	UGC 9851	0.008	J,H,K	2	S0,Sab	MONICA
ngc 5953		0.007	H	2	Sb/	MONICA
ngc 6814		0.003	J,H,K,CO	U1	Sa/	MONICA
ngc 7465	MRK 313	0.006	J,H,K	2	Sa/	MONICA
ngc 7582	ESO 291-g16	0.005	H,K	2	Sa/	MONICA
ngc 7590		0.005	H	2	Sb/	MONICA
ngc 7743		0.007	H,K,CO	2	Sa/S0a	MONICA
ngc 5005		0.002	H	2	S0/	MONICA

4. NGC 3227

The CFHT J,H,K- and HST V-band images are presented in Figure 4 on a log scale. A diffuse, ellongated structure containing wispy spiral bands is seen surrounding the nucleus in all wavelengths. Subtraction of a smooth model reveals that this region is punctuated with bright knotty structures tracing out a mini-spiral pattern within a region 3"x2" (Figure 6). The colours of these knots are consistent with a red supergiant population, with a scattered AGN light contribution near the core. However, the presence of the AOB artifacts in the very core region make the identification of physical knots difficult. We explored several methods of removing the low frequency galactic component, including various smoothing filters, a one-dimensional elliptical isophote model, and a multi-component (bulge+disk+point source) elliptical isophote model. All methods consistently unveil the knotty spiral structure. However, in the central arcsec of the galaxy, subtracting isophotal fitting models results in prominent artifacts which obscure structural details as described in section 3.1.

Color maps are formed by convolving the images to the worse resolution of a given pair and taking the flux ratio (Figure 5). Any color gradients in these images can result from several different processes: 1) change in dust 2) change in stellar population 3) change in gas. The most prominent feature is an irregular-shaped patch to the southwest. The fact that this region appears clearly as a deficit in the V-band image, and takes on a patchy morphology is strong evidence for dust obscuration as the source of the color gradient. The region is therefore most pronounced the V-K color map, since the K image is least affected by dust. The J-K image indicates that substantial dust still affects this region in the J-band. The nucleus is also very red relative to V and J, possibly as a result of thermal dust emission in the K band. The red colors of the knotty spiral starburst stand out from a region slightly bluer than the larger scale bulge of the galaxy.

The images are distorted by PSF artifacts in the central 0.5", with strong diffraction spikes in the HST image. However, there appears to be a disk-like feature most clearly visible in the J-K and V-K color maps, as it seems to be bluer than the rest of the galaxy at K. The position angle of $43°$ indicates that this elongation is unrelated to the AOB artifacts seen in figure 1. The 1D profiles of the galaxies are similar at J, H and K, displaying bumps in ellipticity at 1.5 and 0.5 arcsec radius, confirming the presence and position angle of the above disk and the enhanced region coincident with the spiral starburst. The isophotes are twisted of order $10°$ in both cases.

The images are also compared to the 6cm and 18cm MERLIN radio continuum emission, both of which align with the axis of the nuclear spiral as seen in Figure 6. Previous explanations for the radio structure (Mundell et al 1995), invoked the standard unified AGN model to explain this emission as collimated outflow. However, there is an offset in orientation of the [OIII] "cone" and the small-scale radio features. A projection effect would be possible, but this would necessitate that the NE side of the disc is closer to us than the SW side. This could only occur if the spiral arms were leading rather than trailing (Mundell et al 1995). As figure 6 shows, the radio aligns well with both the orientation and some of the knots of the starburst spiral, and the obvious interpretation is that we are seeing synchrotron emission from SNe remnants.

4.1. Discussion

Several possible scenerios emerge from these results. We tabulate the observed structures in this galaxy from the largest to the smallest in Table 2. On the largest scales Gonzalez Delgado et al. (1997) noted that a large-scale bar appears to transport material towards an inner radius which corresponds to the calculated inner Linblad resonance (ILR) at roughly 7". At this point, prominent dust and HII regions indicate substantial star formation. Within this region, a molecular bar of length $\sim$ 1kpc is observed in CO with and ILR of 2" (Schinnerer 1998). This radius corresponds with the outer extent of the spiral starburst rings in our images.

With such nested bar structure repeating itself at these two larger scales, it is natural to speculate that the small scale elongation seen in the color maps and profile analysis may be yet another bar potential funneling material down to the scales where viscous forces may take over to fuel the AGN. However, a larger scale extended [OIII] region (Arribas et al. 1995) lies to the northeast and has been interpretted as a narrow-line region ionized by the AGN, collimated into a bi-cone by a small-scale ($\sim pc$) dusty torus. The fact that this collimation axis roughly aligns with our "bar" may be an indication that this elongation actually represents scattered AGN light. This is made all the more convincing by the blue colour of the elongation.

On the other hand, if our observed small-scale elongation is some sort of twisted disk as found in Centaurus A by Schreier et al. (1998), its plane lies roughly perpendicular to the axis defined by the radio "jet" observed at 6 and 18 cm, and would be consistent with a collimated radio jet normal to an accretion disk plane. For the radio emission to be interpretted as an outflow, the collimated [OIII] ionization picture would then have to be abandoned. A more detailed analysis can be found in Chapman et al. (1999b).

Table 2

The structural components of NGC 3227

Component	Scale	PA (°)	Ellipticity	Observed with	Function in galaxy
Large Scale galaxy	1-10 kpc	-25	0.5	V-band	
Large Scale bar	1-5 kpc	-45	0.8	galaxy subtracted	funnel material to ILR at 7"
Extended [OIII]	1kpc	35		OIII filter/ OASIS [SIII]	collimated emission?
Circum-nuclear ring	1 kpc			H_α	ILR
Medium Scale bar	100-1000pc	?		submm CO	funnel material to ILR at 2"
K-band ellipse	200 pc	-10	0.2	model subtract/ color maps	spiral starburst, ILR
Radio jets/blob	100 pc	-10		MERLIN 8/16cm	SN/outflow?
K-V blob	100 pc	-10	0.1	K-V map, raw Vband	bluer than galaxy
K-J annulus	100 pc	40	0.3	K-J, K-V, J maps	twisted disk/bars, scattered AGN light

5. NGC 2992

In figure 7, we present an H-band AOB image of the central 7" of NGC 2992. Of obvious note are the jet-like extent to the NW, and the elongated isophotes to the SW along the galaxy disk. The V-band HST image is also depicted with 8.4GHz radio contours overlaid. Although it is still clear that the isophotes are elongated to the SW along the galaxy disk, the galaxy morphology is much more distorted due to the effects of dust and there is no indication of the extension to the NW out of the galaxy plane.

The V-band image shows that the radio emission lying along the galaxy disk has no obvious opical emission associated and appears to lie well within the dust lane. When we form an H-V color map, we now observe highly reddened emission lying along the radio contours in the disk of the galaxy, however with what appears to be a loop to the north, associated with an inner loop of radio emission.

By subtracting a model image consisting of either elliptical fitted isophotes, or a smooth median filtered image, we are able to discern the spiral arms along the disk, as well as an extension to the West (figure 7), also noted in Alonso-Herrero A. et al. 1998. There is clearly some radio emission coincident with the southern spiral arm, which breaks up into a similar knotty morphology to the H-band model-subtracted image. At faint levels, it is also possible to discern knotty features along the northern red H-V loop, the colors of which are consistent with star formation. The extended feature aligns with the beginning of the H-V loop noted above, but continues outward to fill the radio loop.

There is, however, little sign of optical or near-IR counterparts to the radio loops out past the disk of the galaxy, even at K-band where the ability to see through the dust lane is greatest. This is evidence for the actual figure-8 loops lying out of the galactic disk plane, superimposed over fairly strong disk emission related to star formation. If the extended near-IR emission to the West is related to the NW radio loop, the dust lane must extend out past the loop in order to heavily obscure the optical/near-IR emission. This sort of near-IR "jet" may exist towards the SE radio loop as well, although largely obscured by the galaxy disk.

There are several favored models for such figure-8 radio emission. The most convincing in light of our new near-IR imaging is that the loops result from some sort of expanding gas bubbles which are seen preferentially as limb-brightened loops (Wehrle 1988). Such outflows may be associated with the AGN core, which is consistent with the orientation of the proposed ionization cones observed at larger scales Allen et al. 1998. Superwinds in starbursts would blow preferentially out of the galaxy plane, such as in NGC253 (Unger et al. 1987), providing a similar mechanism even without a strong AGN driving the outflow. Here, however, the [OIII] emission is likely to be associated, but not continuum emission thus our data likely rule out this latter model. These possibilities are further explored in Chapman et al. (1998c)

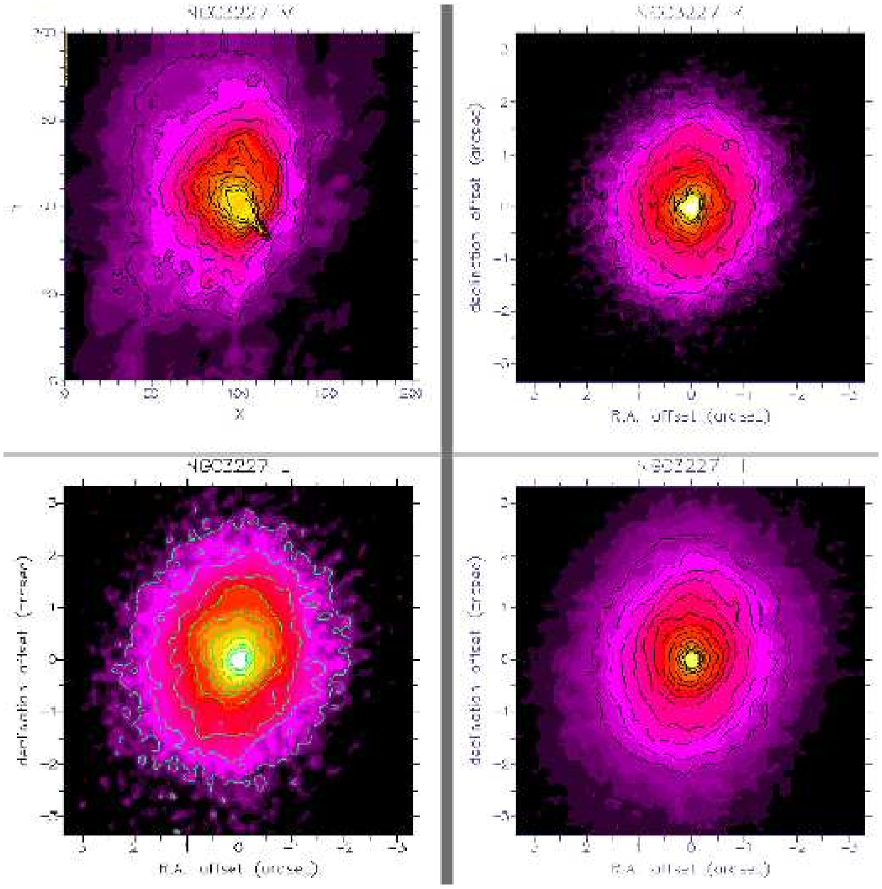

Fig. 4.— Clockwise: ngc 3227 HST F606W and AOB J,H,K images. The AOB images have been deconvolved using the LUCY algorithm with 20 iterations.

REFERENCES

Allen et al. 1998, astro/ph9809123

Alonso-Herrero A., Simpson C., Ward M. J., Wilson A. S., 1998, ApJ, 495, 196

Antonucci R., 1993, A&A Rev.31, 473

Chapman S. & Morris S.L., in preparation 1999a.

Chapman S. & Morris S.L., 1999b, submitted to MNRAS.

Chapman S., Morris S.L., Alonso-Herrero A., Falcke H., in preparation 1999c.

Falcke, H. et al., 1988, AJ, 95, 1689

Arribas S., Mediavilla E. 1994, ApJ, 437, 149

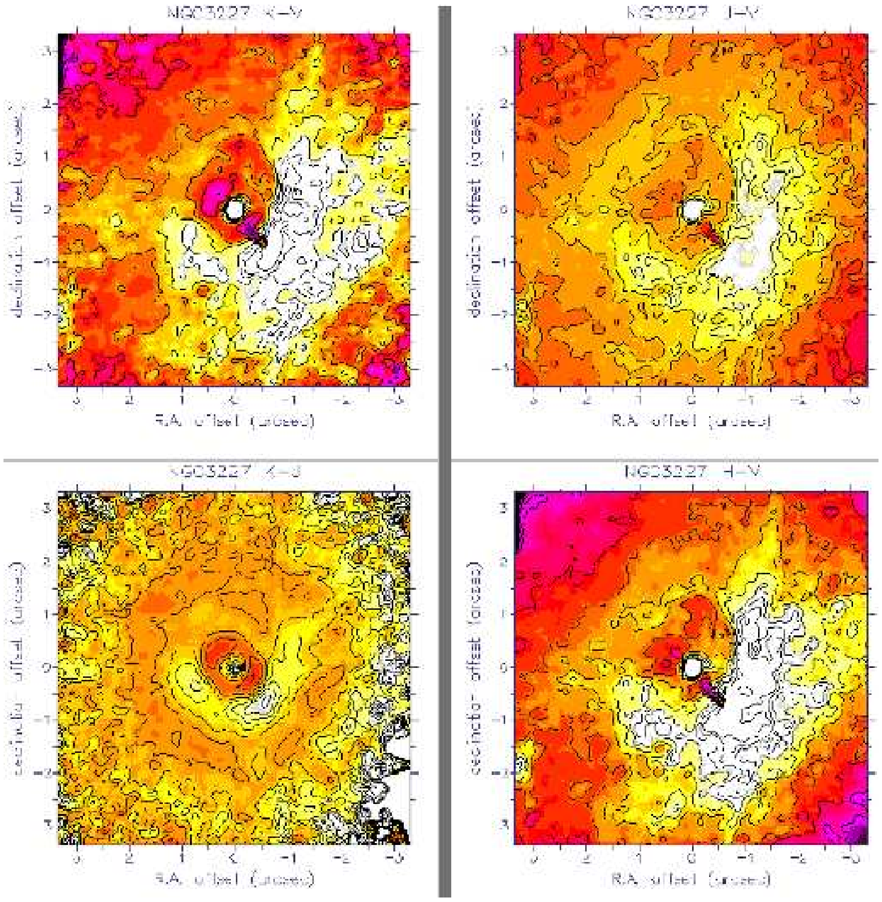

Fig. 5.— ngc 3227 color maps: K-J, K-V, H-V, J-V

Gonzalez Delgado R.M., Perez E. 1997, MNRAS, 284, 931

Knapen J., et al, 1997 MNRAS, 500, 500

Lai O. et al., 1998, A&A, in press.

Mundell C.G., et al. 1995, MNRAS, 275, 67

Nadeau D., Murphy D.C., Doyon R., Rowlands N., 1994, PASP106, 909

Roddier F.J., Graves J.E., McKenna D. , Northcott M.J. , 1991, Proc. SPIEVol. 1524, p. 248

Rouan D. et al., 1998, A&A, in press.

Schreier E.J. et al. 1998, ApJ, in press

Schinnerer E. et al. 1998, AGM 14, H08

Ulvstad & Wilson A. 1984,

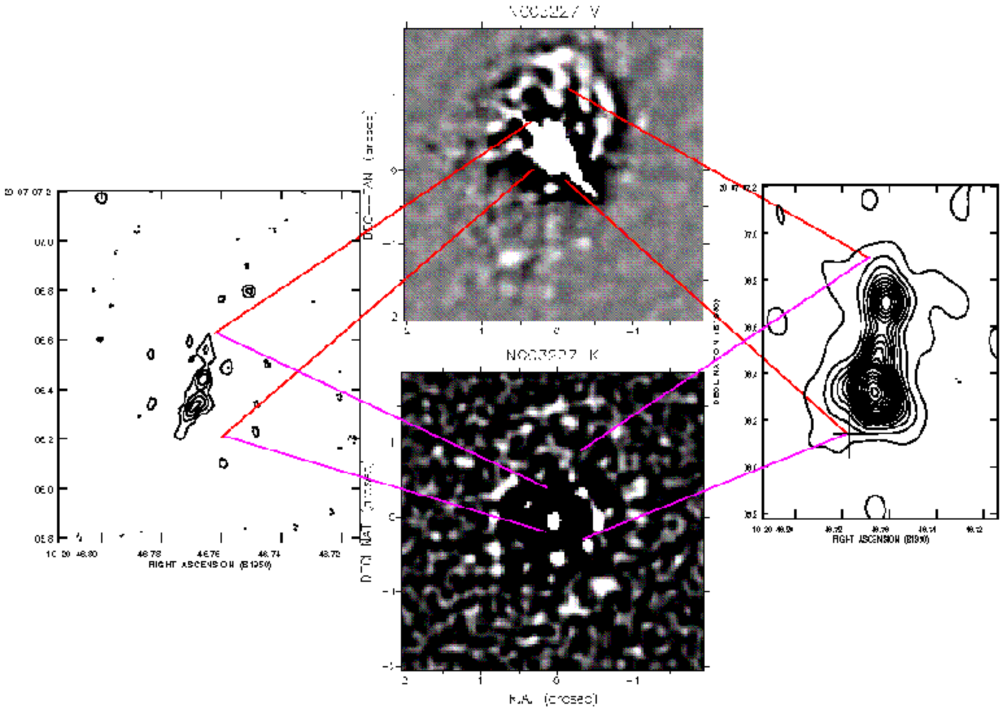

Fig. 6.— ngc 3227 model subtracted images (Top: V-band, Bottom: K-band 4” on a side), with MERLIN radio contours to right (18cm) and left (6cm). The 18cm peaks appear to align with the galaxy core and a starformation knot to the north.

UNGER, S. W., PEDLAR, A., AXON, D. J., WHITTLE, M., MEURS, E. J. A., WARD, M. J., 1987 MNRAS, 228, 671

Veran J.P., Rigaut F., Maître H., Rouan D., 1997, Journ. of the Optic. Soc. of America A 14, 11

Wehrle A. E., Morris M., 1988, AJ, 95, 1689

This preprint was prepared with the AAS LaTeX macros v4.0.

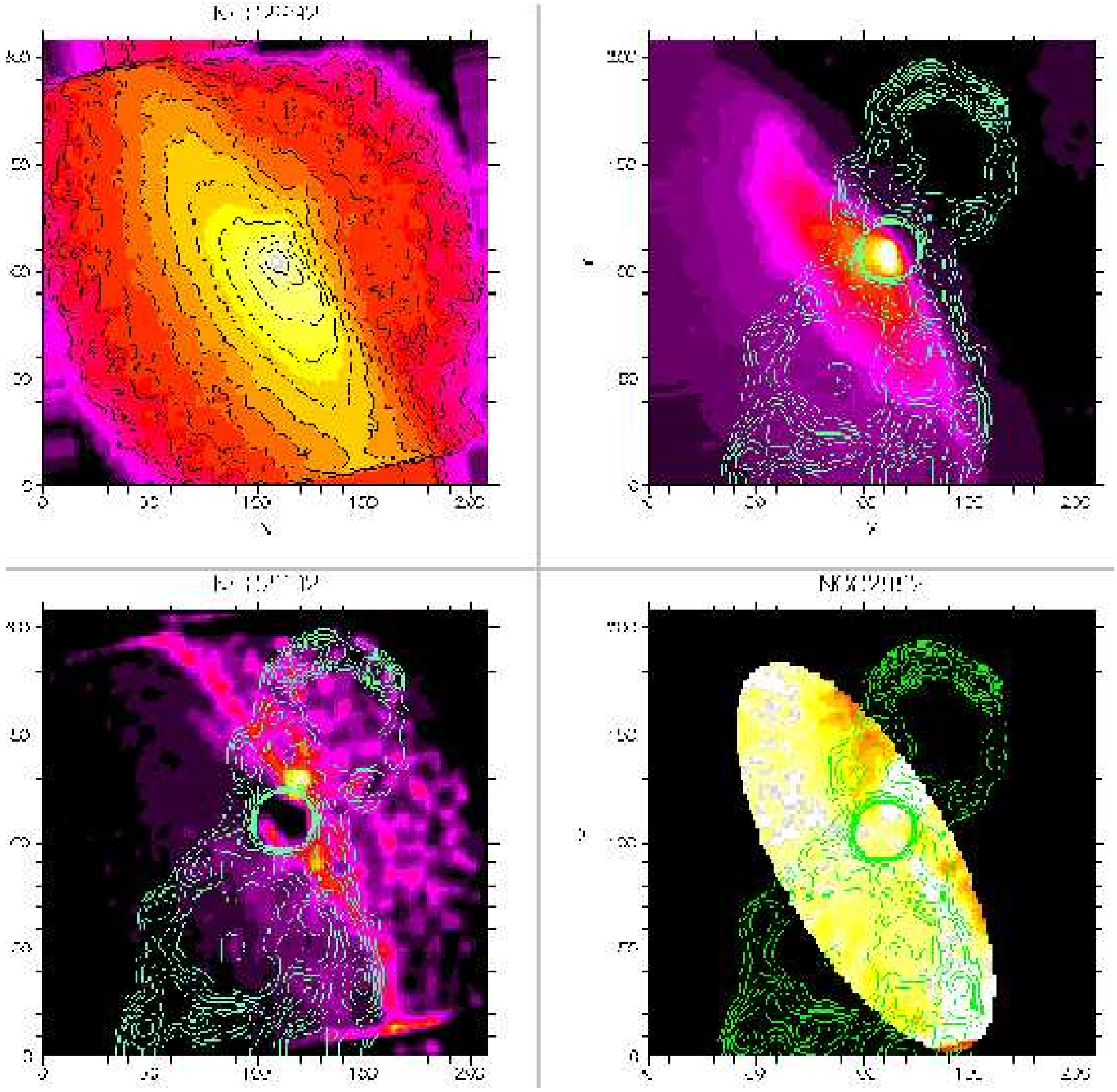

Fig. 7.— Clockwise: a) NGC 2992 H-band, 7” on a side; b) V-band HST image with 8.4GHz radio contours overlay; c) H-band smooth model subtracted; d) H-V color map: red is bright at H-band.